J. Membrane Biol. 14, 305–338 (1973)

The Relationship between ATP and an Electrogenic Pump in the Plasma Membrane of *Neurospora crassa*

C. L. Slayman, W. S. Long, and C. Y.-H. Lu

Department of Physiology, Yale University School of Medicine, New Haven, Connecticut 06510

Received 9 August 1973

Summary. Sudden respiratory blockade has been used to study rapid changes of the resting membrane potential, of intracellular adenosine 5′-triphosphate (ATP) levels, and of pyridine nucleotide reduction in *Neurospora crassa.* Membrane depolarization occurs with a first-order rate constant of 0.167 sec^{-1}, following a lag period of about 4 sec, at 24 °C (ambient temperature). This depolarization is several-fold too slow to be directly linked to electron transfer, as judged from the rate of pyridine nucleotide reduction, but has essentially the same rate constant as the decay of ATP. The latter process, however, shows no lag period after the respiratory inhibitor is introduced. Plots of membrane potential versus the intracellular ATP concentration yield saturation curves which are readily fitted by a Michaelis equation, to which is added a constant term representing the diffusion component of membrane potential. Parameters obtained from such fits indicate the maximal voltage which the pump can develop at high ATP levels to be 300 to 350 mV, with an apparent $K_{1/2}$ of 2.0 mM. The data strongly suggest that an electrogenic ion pump in the plasma membrane of *Neurospora* is fueled by ATP; comparison of the measured membrane potentials with the energy available from hydrolysis of ATP indicates that two ions could be pumped for each molecule of ATP split.

Although the existence of electrogenic ion pumps was postulated about 50 years ago from extracellular studies on plant tissues and on epithelial membranes, their acceptance as *bona fide* physiological entities did not occur until the past 10 years. During this period proof has been evolving from two quite separate lines of research. First, in certain nerve and muscle preparations, where membrane potential and resistance can be measured with micropipette electrodes, it has been possible to demonstrate a precise quantitative correspondence between the currents (and fluxes) generated by the sodium pump and the voltage and resistance characteristics of the particular membrane [2, 18, 23, 33, 51, 52]. Related experiments on plant and fungal preparations have given less complete data, but have clearly demonstrated the existence of membrane potentials which are extremely difficult to account for in terms of conventional ion-diffusion processes

[12, 18, 19, 35, 39, 48]. Second, in energy-conserving membranes – i.e., mitochondria, chloroplasts, and bacteria – a large body of evidence has accumulated to indicate the presence of ionic movements and, indirectly, large membrane potentials which are intimately associated with the process of energy conservation [26, 37].

In energy-conserving membranes the oxidation-reduction reactions of electron transfer are postulated to drive (or constitute) electrogenic ion pumps [26, 27], but it is reasonable to suppose that most other electrogenic pumps are driven by the energy of phosphate bond hydrolysis in nucleoside triphosphates, particularly ATP. This energy lies in the range of 7 to 12 kcal/mole, or 300 to 500 mV. But the actual maximal voltage that a given electrogenic pump can sustain also depends upon the stoichiometry of pump action, and the general conductance or leakiness of the particular membrane. For leaky membranes, as are usually encountered in animal tissues, the maximal voltage lies in a low range: 75 to 150 mV (but *see* Tamai & Kagiyama [50] for an exception); for energy-conserving membranes, in the range 150 to 250 mV; and for plant and fungal membranes in a somewhat higher range still: up to 300 mV. The principal ions which are known or suspected to be electrogenically pumped are sodium, in nerve, muscle, and a variety of epithelial membranes [18, 32, 52]; chloride, in some epithelial membranes [11, 18, 31] and in plant cells [12, 35]; and hydrogen ions, in the energy-conserving membranes [14, 26, 37], in the gastric mucosa [31, 32], and in plant and fungal cells [19, 40, 48].

Among electrogenic pumps, the putative hydrogen ion pump driven by energy from ATP hydrolysis may hold a unique position. Its main role in energy-conserving membranes would be to run backwards, down the electrochemical gradient for H^+ ions, to accomplish the synthesis of ATP [27, 37]; but in membranes (especially certain bacterial, fungal and plant plasma membranes) which cannot carry out electron transfer, it has been postulated to function in the forward direction, to generate a membrane voltage which might in turn be used to distribute energy to other transport processes [14, 27, 44], perhaps via ion co-transport systems [44, 57]. Unfortunately, all evidence thus far reported supporting the existence of such an electrogenic pump is indirect: massive amounts of data on H^+ flux and ATP hydrolysis by the energy conserving membranes have not yet been supported by direct measurements of membrane voltage and resistance; and electrical measurements on plant and fungal cells have not yet been supported by adequate studies on H^+ movement or metabolism.

It is therefore the primary purpose of this report on the fungus *Neurospora* to present data strongly linking the membrane voltage generator to the

breakdown of intracellular ATP. The data discussed have all been obtained during transients at the onset or release of respiratory inhibition. A subsequent paper will present complementary data obtained under quasi steady-state conditions. A preliminary report of the present results has already appeared [42].

Materials and Methods

General

The wild-type strain RL21a of *Neurospora crassa* was used throughout these experiments. Details of the methods for growing and handling the fungus have been described previously [38, 46]. For chemical measurements of ATP levels, fluorescence, or respiration, shaking liquid cultures were grown for 15 to 16 hr at 25 °C [46]. Cultures were then harvested on cheesecloth, rinsed several times with distilled water, resuspended at a density of 1 to 2 mg dry wt/ml in buffer, and allowed to preincubate 20 to 90 min at 25 °C before use. For electrical measurements mycelial colonies were grown 20 to 36 hr on scratched cellophane supported by 3 % agar, also at 25 °C [38]. For recording, a piece of cellophane with the attached section of colony was removed from the agar, rinsed thoroughly in distilled water, and transferred to a Lucite chamber on the stage of a compound microscope. The chamber was similar to that described previously [39], except that its sides were open and solution was removed by a vacuum level-regulator.

Throughout the experiments to be discussed, the important comparisons are between chemical measurements (mostly ATP) made on the small cells from shaking cultures and electrical measurements made on the large mature hyphae from stationary cultures. The validity of the interpretations, therefore, depends upon reliable extrapolation of at least one kind of measurement to the other kind of cell. Shaking-culture cells are simply too small (2 to 3 μ diameter) for microelectrode studies, and segments of individual mycelial hyphae are likewise too small for measuring ATP with present techniques, so the main experimental test of reliable extrapolation is measurement of ATP decay in masses of mycelium. This experiment, carried out in conjunction with a more detailed study of adenine nucleotide metabolism in *Neurospora* [41], demonstrated exponential decay of ATP upon sudden blockade by cyanide, with a rate constant of $0.172 \pm 0.016\ \text{sec}^{-1}$ for the mycelium, and $0.176 \pm 0.020\ \text{sec}^{-1}$ for the shaking-culture cells. The data were more scattered, and the net change in ATP concentration was smaller, however, in the mycelium; both of these differences probably arise from cell heterogeneity in the mycelial colonies.

Solutions

The medium described by Vogel [55] was used for growing all cells, but since *Neurospora* maintains high and stable ATP levels and membrane potentials in much less complicated solutions, simple buffers or saline solutions were adopted for most of the measurements. These are listed in Table 1. Except as otherwise noted, all chemical experiments were carried out at 25.0 ± 0.1 °C, and all electrical experiments at 24 ± 1 °C (ambient temperature).

Fluorescence Measurements

A number of preliminary measurements as well as the experiment in Fig. 10*A*, were carried out (with the aid of Mr. Brian Paddle) on a differential fluorometer designed by

Table 1. Compositions of solutions

Solution	K^+ (mM)	Anion (mM)	$CaCl_2$ (mM)	pH	Sugar (%)
A	10	Cl, 10	1	5.8[a]	Sucrose, 2
B	50	Phosphate, 45.6	0	5.8	Glucose, 1
C	25	DMG[b], 20	0	5.8	Glucose, 1
D	25	DMG, 20	1	5.8	Glucose, 1
E[c]	10	Phosphate, 9.1	1	5.8	Glucose, 1
F	25	DMG, 4; Cl, 20	1	5.8	Glucose, 1
G	25	DMG, 20; KCN, 25	1	5.8	Glucose, 1

[a] This is the pH of Vogel's growth medium and, coincidentally, of distilled water in equilibrium with air.
[b] 3,3-dimethylglutaric acid; it has pK's of 3.66 and 6.20, and is essentially inert for *Neurospora* [43]; made up as the acid, with 25 mM KOH added.
[c] This medium contained in addition 0.5 mM $MgCl_2$, 1 mM NH_4NO_3, and biotin and trace elements as in Vogel's medium.

Dr. Britton Chance, at the Johnson Foundation, University of Pennsylvania. The instrument was calibrated with free NADH in solution, which was assumed to have its emission maximum at 485 nm [4], and displayed a half bandwidth of 80 nm. The characteristic fluorescence of *Neurospora*, illuminated at 360 nm, was determined by comparing nitrogen- or cyanide-reduced cell suspensions with well-aerated suspensions. In both cases the resultant difference spectrum had its maximum at 482 nm, and a half bandwidth of 72 nm.

In routine experiments, fluorescence was recorded with an Aminco-Bowman spectrophotofluorometer (American Instrument Co., Silver Spring, Md.) using an exciting beam at 360 nm and measuring emission at 485 nm (3 mm slits). On the basis of the spectra reported above, increases in the measured fluorescence upon introduction of potassium cyanide were assumed to represent the reduction of NAD^+ and $NADP^+$. The mechanical arrangement for the measurements was as follows. Two milliliters of cell suspension, in a quartz cuvette, were placed into the fluorometer; the cuvette chamber was fitted with two syringe ports: one for passage of a steady stream of oxygen bubbles, which kept the cells mixed and suspended as well as oxygenated, and one for injection of inhibitor. At zero time, 0.2 ml of neutralized KCN was injected, to a final concentration of 80 to 100 mM. The short time constant for the primary fluorescence response, about 1 sec (*see* Results, *below*), demanded a test of instrument response time (for mixing and recording); injection of NADH or India ink revealed this to be about 0.2 sec, which can be considered negligible in view of the excess of cyanide used over the minimum blocking concentration (1 to 3 mM).

ATP Analyses

The method for rapid measurement of ATP levels in *Neurospora* has been detailed in a previous publication [41]. It was based on the firefly luciferase assay of Strehler [49], and involved harvesting the cells into petroleum ether/dry ice, lyophilizing overnight, and extracting the pellets with perchloric acid. Flashes were measured with the photomultiplier of the fluorometer *(see above)*.

Electronic Apparatus

Solid-state electrometer amplifiers designed by Mr. H. Fein (Model M-4, W. P. Instruments, Hamden, Conn. [8]) were used for recording the potential difference between the cytoplasm of *Neurospora* and the external solution. The devices have an input impedance greater than 10^{10} ohms and a leakage current of 5×10^{-12} amp. The microelectrodes *(see below)* and ground electrode were filled with 3 M KCl and were led to the amplifier via matched Ag-AgCl half-cells. Signals from all amplifiers were led to an oscilloscope and to a chart recorder.

Microelectrodes

Glass micropipettes with tip diameters less than 1 μ were produced on an ISA puller (Industrical Science Assoc., Ridgewood, N.Y.) and were filled, by vacuum boiling (90 to 95 °C), with 3 M KCl. They had resistances greater than 5 MΩ when measured with their tips in 3 M KCl. End taper was found to be crucial in obtaining microelectrodes that would penetrate *Neurospora* without either tearing the membrane and the wall or breaking the pipette tip, so that tip shape was routinely monitored in the light microscope (400×). Measurements of the intracellular potential of *Neurospora* were adjusted for the tip junction potential of the electrode, according to a procedure described previously [38], but the average correction in the present experiments was small (ca. 5 mV).

Mixing Characteristics of the Flasks and Chambers used for ATP and Voltage Measurements

For ATP measurements 20-ml cell suspensions were kept in 125-ml flasks, on a reciprocating shaker at 140 cycles/min. Inhibitors were injected rapidly in a volume of 2.2 ml. The high rate of shaking makes likely an effective mixing time on the order of 1 sec, which is consistent with the facts (*see* Fig. 3*A*) that no discernable lag was apparent in the decay of ATP and that the shape of the decay curve was not dependent upon inhibitor concentration.

In the electrical experiments inhibitors were added by perfusing solution through the recording chamber. Maximal flow through the chamber was limited—because of mechanical disturbances arising from the branched structure of *Neurospora*—to about 9 chamber-volumes per min (15 ml/min, compared with a chamber volume of 1.7 ml). Solution exchange in the vicinity of several test cells was estimated from the shift in tip potential of an extracellular microelectrode, produced by switching from 10 mM KCl to 25 mM KCl; at 9 chamber-volumes per min exchange was approximately exponential, with a time constant of 4 sec. Since this time constant was close to that expected for the physiological voltage change, a rather high concentration of inhibitor (25 mM KCN) was used in routine experiments, to bring the local inhibitor concentration up to the minimal blocking level (1 to 3 mM) in a negligibly short time. For 25 mM KCN, with a time constant of 4 sec, 1 to 3 mM should have been reached in 0.16 to 0.5 sec. In a few cases 5 mM KCN was used for perfusion, and that should have brought the local concentration to 1 to 3 mM in 0.8 to 3.6 sec.

Computations and Plots

All nucleotide data were obtained in units of mmoles/mg dry weight of cells. This was converted to mmoles per kg intracellular water (mM) with the ratio intracellular

water/dry weight = 2.54 [46]. All averages are expressed as the mean ± 1 SEM. Parameter estimation and curve-fitting were carried out on the IBM 370 computer at the Yale Computer Center, using a nonlinear least-squares algorithm [24], and all results are bracketed with ±1 standard error. Voltage records are reproduced with negative voltages (cell interior) downward, according to the usual electrophysiological convention (Figs. 2, 12). Voltage plots are shown with negative values upward, to facilitate comparison with chemical data.

Results

Comparison with Electron Transfer

The cardinal property of the resting membrane potential of *Neurospora* which suggests the existence of an electrogenic ion pump is the speed with which depolarization occurs upon treating the cells with respiratory inhibitors: absolute rates approaching 20 mV/sec, with a first-order rate constant of 0.185 sec^{-1} [42]. This compares with an average rate constant for potassium loss of 0.032 min^{-1}, or 0.00053 sec^{-1} (calculated from [47]). The question naturally arises whether this rapidly shifting membrane potential could arise directly from respiratory electron transfer, as has recently been implied for mitochondrial and chloroplast membranes [37]; or whether energy must be transferred to the pump via an energy shuttle, such as ATP. The latter alternative would be more reasonable for the plasma membrane of eukaryotic organisms, which have not been found to contain measurable quantities of the respiratory electron transfer system. This argument alone is not compelling, however, since at least one other ion transport process presumed to reside in the plasma membrane – chloride transport in the giant algae [22, 29, 30] – appears more closely tied to electron transfer (photoelectron transfer) than to phosphate bond energy.

In the case of *Neurospora*, it is possible to test the question of a direct role for respiratory electron transfer in generating the membrane potential, by comparing the rate at which cyanide blockade shuts down electron transfer with the rate at which the membrane potential decays. A very conservative estimate of the rate at which electron transfer ceases can be obtained by measuring the reduction of total intracellular pyridine nucleotides. The molecular ratios of total pyridine nucleotides (PN), to mitochondrial pyridine nucleotides, and to other components of the electron transfer chain in *Neurospora* are listed in Table 2. Given the great excess of PN, the cytochromes and flavoproteins would be expected to reduce much more rapidly than PN during respiratory blockade. This expectation has been verified in the case of liver mitochondria by Chance and Williams [6]; at the onset of anoxia, the calculated rate constants for reduction of the successive com-

Table 2. Molecular ratios of respiratory electron carriers in *Neurospora*

Carrier	Ratio
Cytochrome aa_3	≡1.0
Cytochrome *b*	1.0
Cytochrome *c*	4.2
Mitochondrial flavoprotein	2.9
Mitochondrial pyridine nucleotide	35
Cytoplasmic pyridine nucleotide	100

All values except that of cytoplasmic pyridine nucleotide are taken from [20]. Cytoplasmic pyridine nucleotide was estimated from the data of Brody [5] and Zalokar [58], assuming that total protein/dry weight = 0.5.

ponents of the respiratory chain are as follows: cytochrome *c*: 0.12 sec^{-1}; cytochrome *b*: 0.12 sec^{-1}, flavoprotein: 0.058 sec^{-1}, PN: 0.025 sec^{-1}.

Since the reduced pyridine nucleotides, NADH and NADPH, fluoresce but the oxidized nucleotides do not, the rate of change of fluorescence intensity measures the rate of NAD^+ and $NADP^+$ reduction [4]. The average time course of the fluorescence increase in response to the sudden injection of KCN into a suspension of shaking-culture cells is shown in Fig. 1. In all trials the fluorescence curve appeared to contain two exponential components: a large fast component which was always in the direction of PN reduction, and a smaller slow component which was usually in the same direction (Fig. 1, Inset *A*), but occasionally appeared as PN oxidation (Fig. 1, Inset *B*). The average curve can be described by the empirical equation:

$$\text{Fluorescence} = A_1(1-e^{-k_1 t}) + A_2(1-e^{-k_2 t}), \tag{1}$$

and the least-squares fit of the data in Fig. 1 to this equation yields rate constants of 0.600 ± 0.073 sec^{-1} and 0.124 ± 0.014 sec^{-1} for the fast and slow components, respectively. The two components are shown separated in Inset *C* to Fig. 1. (A single-exponential fit to these average fluorescence data gives a fourfold larger sum of squared deviations.) It is tempting to regard the initial, stable, fast component of the fluorescence change as reflecting the primary process of pyridine nucleotide reduction; and to assign the second, less stable, and slower component to other events, such as adjustment in the glycolytic pathway or spurious binding of cyanide.

A direct comparison between the fluorescence curve and several voltage traces is shown in Fig. 2. In each quarter of the figure an individual voltage trace is reproduced, as well as both the fast component of the fluorescence curve and the overall average curve, all scaled to the same total change.

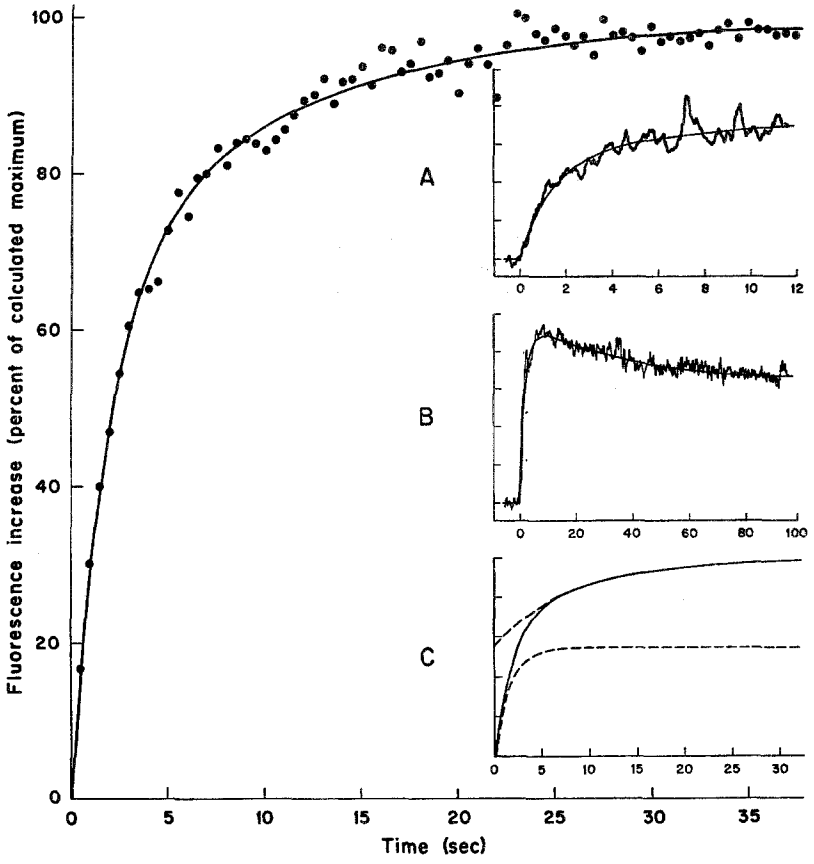

Fig. 1. Time course of fluorescence increase following addition of cyanide to aerobic suspensions of *Neurospora.* Cells suspended in solution D and bubbled with oxygen; 1 M KCN at pH 7.5 injected at zero time, to final concentration of 80 to 100 mM. Excitation 360 nm, emission 485 nm, 3 mm slits. Ambient temperature, ca. 22 °C. *Main Figure:* plot of time-average data for 41 trials. *Inset A* and *Inset B:* two of the fluorescence records contained in the average plot, showing rising (*A*) and falling (*B*) slow components. *Inset C:* separation of the two components in the average curve. (Note the different time scales in the Insets.) All curves fitted by least-squares [24] to the sum of two exponentials [text Eq. (1)], with the following parameters:

Curve	Parameter			
	A_1 (%)	A_2 (%)	k_1 (sec^{-1})	k_2 (sec^{-1})
Average	55.1 ± 5.3	44.9 ± 5.0	0.600 ± 0.073	0.124 ± 0.014
Inset *A*	57.2 ± 3.4	42.8 ± 13.7	0.642 ± 0.083	0.026 ± 0.018
Inset *B*	100 ± 2	-41.4 ± 1.2	0.388 ± 0.016	0.026 ± 0.003

The four voltage traces represent the fastest observed responses of the membrane potential to cyanide inhibition. Thus, even the fastest voltage shifts were slow by comparison with the rate of pyridine nucleotide reduction in

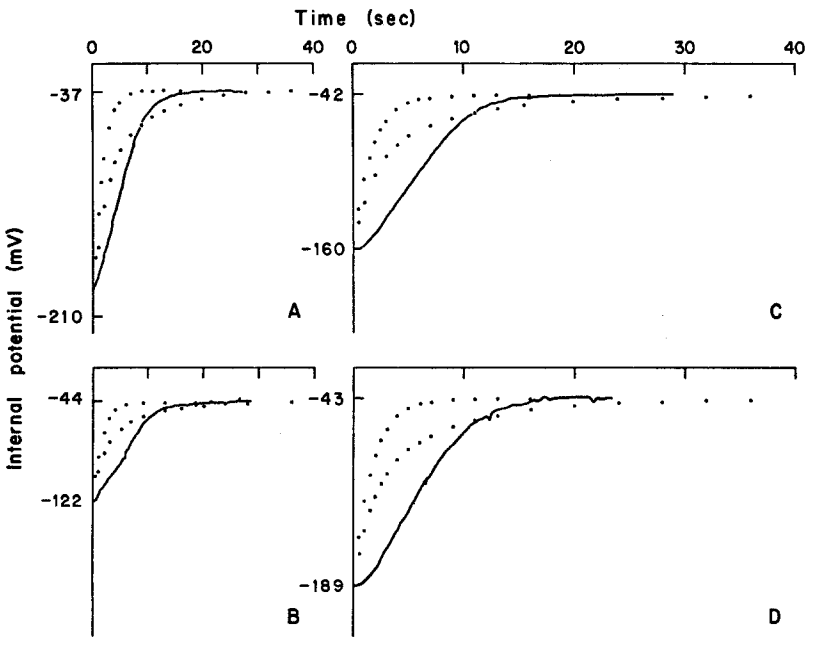

Fig. 2. Individual voltage responses to cyanide, compared with average fluorescence curves. The solid traces represent the four fastest voltage responses which have been observed; the dotted curves in each part of the figure represent either (upper plot) the fast component of the average fluorescence curve of Fig. 1 ($A_1=55.1\,\%$, $k_1=0.60\,\mathrm{sec}^{-1}$) or the entire fluorescence curve (lower plot), each scaled to equal the total voltage change. In parts *A* and *B* the hyphae were bathed in solution D (Table 1) until zero time, when solution G was washed through; in parts *C* and *D* the hyphae were bathed in solution E, and 5 mM KCN (neutralized) was added to that at zero time. Note the expanded time scales in parts *C* and *D*, compared with parts *A* and *B*

response to cyanide, regardless of whether the whole fluorescence curve or only the fast initial component is assumed to be relevant. Furthermore, when the expected fivefold more rapid reduction of flavoproteins or cytochromes is considered, it becomes clear that the cyanide-induced depolarization occurs too slowly to be directly coupled to electron transfer anywhere in the respiratory chain.

Behavior of ATP at the Onset of Respiratory Blockade

Breakdown of intracellular ATP with respiratory inhibition occurs considerably more slowly than does reduction of pyridine nucleotides. The average intracellular ATP concentration, given as a function of time after injection of cyanide or azide into a shaking cell suspension is plotted in Fig. 3*A* for each of seven different experiments. Each individual curve was

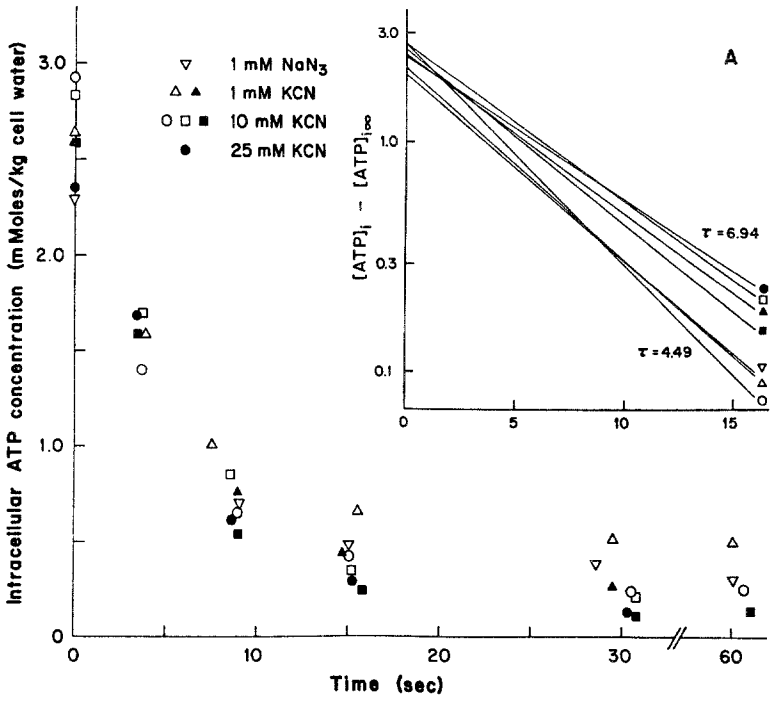

Fig. 3*A*

Fig. 3. (*A*) Summary of time courses of intracellular ATP in response to cyanide and azide. Plots of individual experiments, on linear and semilogarithmic (inset) coordinates; each point plotted represents the average for three measurements. The lines drawn in the inset were fitted by least-squares to a single declining exponential function [text Eq. (2)], and have the following rate constants (k, in units of sec^{-1}): ○, 0.223 ± 0.011; △, 0.194 ± 0.009; ▽, 0.187 ± 0.014; ■, 0.175 ± 0.016; ▲, 0.159 ± 0.012; □, 0.158 ± 0.009; ●, 0.144 ± 0.035. $\tau = 1/k$, in sec. Neutralized KCN or NaN_3 was added at zero time to the cells suspended in solution C (△, ▽, ▲) or solution D (○, ●, □, ■). 25 °C. (*B*) Summary of the time course of intracellular ATP in response to cyanide and azide. Plot of the averaged data for all seven experiments shown in Fig. 3*A*. Curve fitted by least-squares to a single exponential function [text Eq. (2)], and given by $[ATP]_i = 0.26 + 2.36\, e^{-0.175t}$. $\tau = 1/k$, in sec. Vertical bars, ±1 SEM

fitted well by a simple exponential function,

$$[ATP]_i = A_1 + A_2\, e^{-kt}, \tag{2}$$

and the seven rate constants spread between 0.144 and 0.223 sec^{-1} (time constants between 6.94 and 4.49 sec), as illustrated in the inset to Fig. 3*A*. The best-fit rate constant for all data was $k = 0.175 \pm 0.012\ sec^{-1}$ (time constant = 5.72 sec), and a plot of the resulting curve, superimposed on ATP values averaged at each time point, is shown in Fig. 3*B*. In all cases

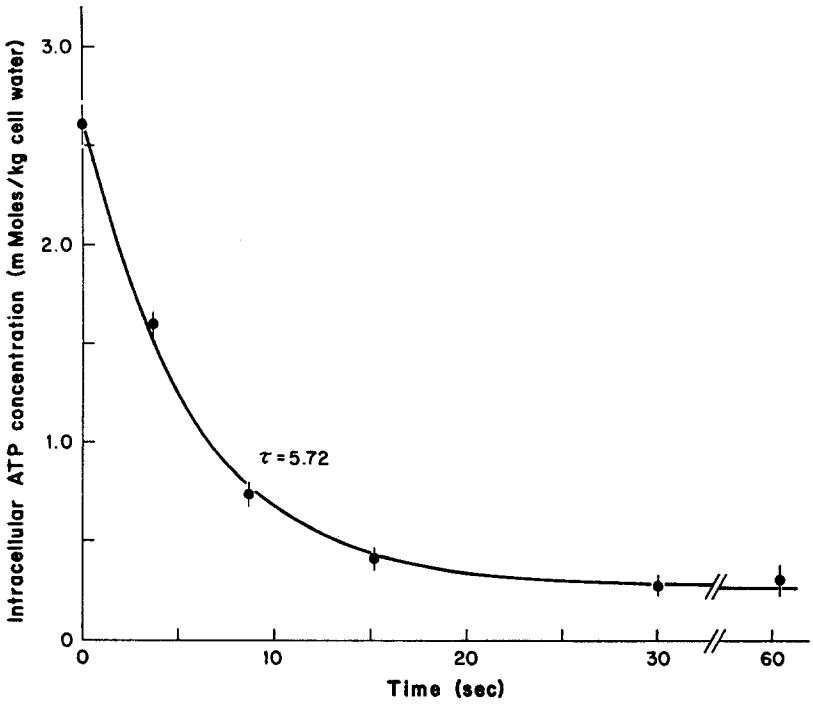

Fig. 3*B*

a small pool of ATP was uninfluenced by the inhibitor: on the average, $A_1 = 0.26 \pm 0.04$ mM, compared with the inhibitor-sensitive fraction: $A_2 = 2.36 \pm 0.06$ mM.

The equivalent experiment on the membrane potentials of mature hyphae was performed by suddenly perfusing 25 mM potassium cyanide solution through the recording chamber. The resulting voltage time course, averaged for 23 trials on 16 preparations, is plotted in Fig. 4*A* (dashed curve). The plot displays an initial phase, several seconds in duration, in which voltage (V_m) declines relatively slowly, followed by a second phase in which the decline appears roughly exponential with time. In fact, the second phase (beginning after 4 sec) can be quite satisfactorily fitted by Eq. (3), using a *rate constant calculated from the ATP data:*

$$V_m = A_1 + A_2 e^{-kt} = 47.4 + 192.9 e^{-0.167t} \quad \text{(in mV)}. \tag{3}$$

The rate constant, 0.167 sec^{-1}, was adjusted (*see* Fig. 6, *below*) from the value of 0.175 sec^{-1} actually observed with ATP, to allow for the slightly lower temperature (24 °C, instead of 25 °C) of the voltage experiments. The

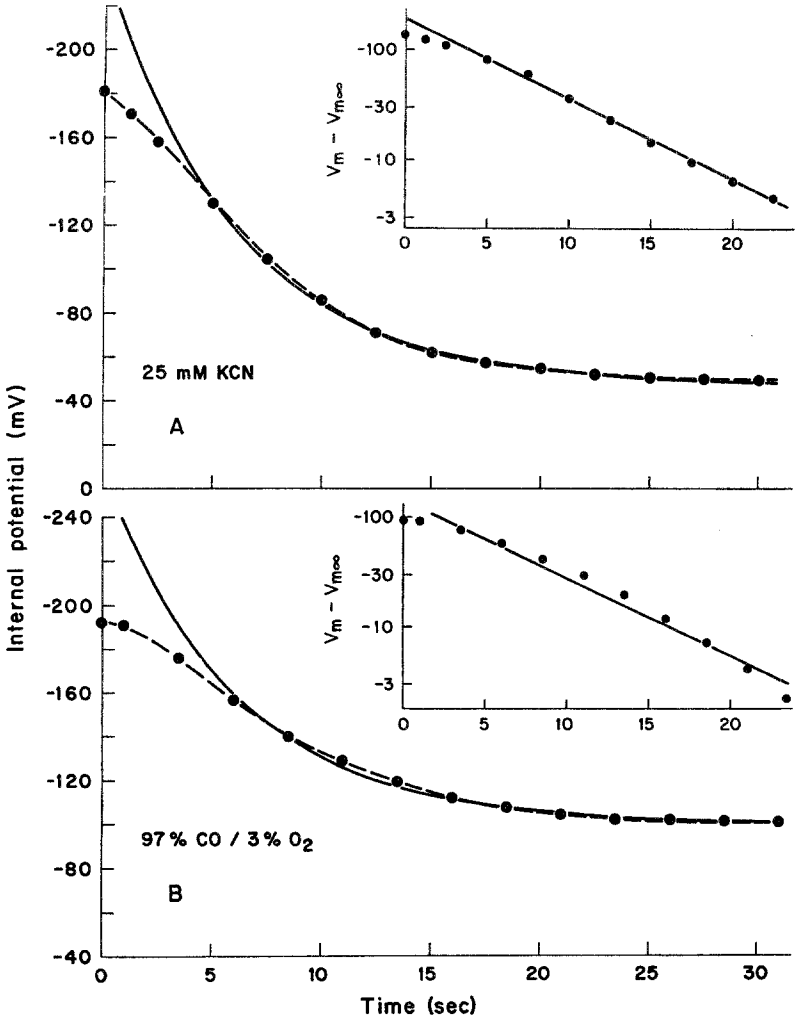

Fig. 4. Time-average plots of membrane potential at the onset of cyanide (*Part A*) or carbon monoxide (*Part B*) inhibition. *A* represents data read from the records for 23 trials on 16 different hyphae bathed in solution D, with solution G substituted at zero time. *B* represents data from six trials on one hyphae bathed in solution D, saturated with 97% CO/3% O_2, but maintained in a bright light; the light was interrupted by a fast shutter at zero time. Average SEM for points in *A*: 4 mV; in *B*: 2 mV. Ambient temperature, ca. 24 °C. The dashed curves were drawn by eye through the points. The solid curves were fitted by least-squares to a single decaying exponential [text Eq. (3)], with the rate constant taken from the ATP data of Fig. 3*B* (adjusted slightly for temperature; *see text*). Points prior to 5 sec were excluded from the fits. Resultant parameters are as follows:

	A_1 (mV)	A_2 (mV)	k (sec^{-1})
Part A	47.4±0.6	192.9±4.9	0.167
Part B	97.1±0.9	136.2±5.6	0.167

Insets show semilogarithmic plots of the same results. V_m = total membrane potential = $A_1 + A_2\, e^{-kt}$; $V_{m\infty}$ = stabilized value of V_m after addition of inhibitor = A_1

semilogarithmic plot (inset) in Fig. 4*A* emphasizes that, after the initial slow phase, the time course of depolarization is indistinguishable from that of ATP decay.

A similar result was obtained from voltage studies with carbon monoxide. This inhibitor blocks respiration at the same site as does cyanide (cytochrome a_3 [10]), but has the advantage that the inhibitor complex is readily dissociated by visible light. Thus, flash illumination of the cells can effectively admit or remove the inhibitor without the delay of fluid exchange. Rapid switching of the light in the present experiments was accomplished by interposing a magnetic shutter (closure time, 10 msec) between the microscope lamp and the stage condenser. The control membrane potential was recorded in solution saturated with 97% CO/3% O_2, and illuminated with a tungsten lamp sufficiently bright to give the maximal steady-state voltage. Fig. 4*B* shows the average time course of membrane potential when the shutter was closed. Although the steady-state depolarization in the dark was not as great with the CO/O_2 mixture as with 25 mM cyanide, the shape of the CO curve is clearly very close to that with cyanide. Again, the solid curve in Fig. 4*B* fits the voltage to an exponential equation with the rate constant 0.167 sec^{-1}:

$$V_m = 97.1 + 136.2\, e^{-0.167t} \quad \text{(in mV)}. \tag{4}$$

Although there is a systematic deviation up to 15 sec (*see* especially Inset, Fig. 4*B*), that deviation is small; and agreement between the predicted curve and the data plot seems generally satisfactory for all times after 5 sec.

This experiment brings out one additional feature of the voltage curves which could not be checked with cyanide: a finite delay between shutter closure (timed electronically) and the first perceptible shift (0.5 mV) of membrane potential. In 38 trials on two cells this delay averaged 0.90 ± 0.07 sec.

Effect of Temperature on ATP and Voltage Transients

If the precise correlation between the time course of ATP decay and that of membrane depolarization in response to cyanide is physiologically significant, then a similar correspondence ought to be observed no matter what the actual rate of ATP decay happens to be. The most convenient way to alter the rate of ATP decay at the onset of respiratory inhibition is to lower the temperature. It has already been shown that lowered temperature *per se* has little effect on steady-state ATP levels in *Neurospora* [41]. For present purposes, ATP curves were determined at two temperatures other

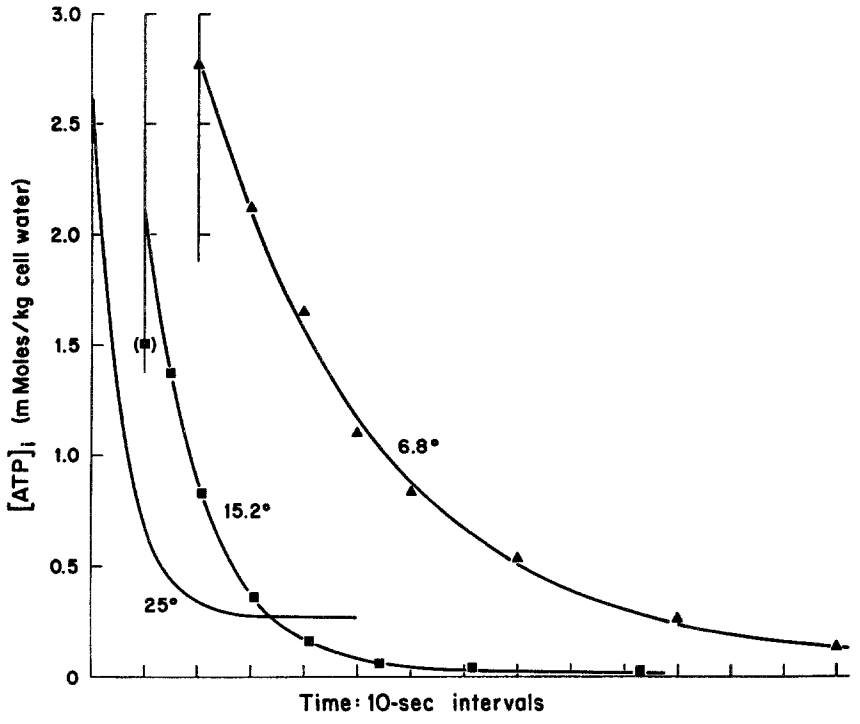

Fig. 5. Temperature effect on the time course of ATP decay with cyanide inhibition. All points plotted are averages for three simultaneous determinations; average SEM for first three points at 15.2 °C: 0.40; for all other points: 0.04. The curves were fitted by least-squares to a single declining exponential [text Eq. (2)], with these resultant parameters:

	A_1 (mM)	A_2 (mM)	k (sec^{-1})
6.8 °C	0.06±0.04	2.74±0.06	0.030±0.002
15.2 °C	0.02±0.01	2.09±0.02	0.088±0.002

Curve for 25 °C is redrawn from Fig. 3*B* for comparison. Cells suspended in solution D, with 10 mM KCN (neutralized) injected at zero time

than 25 °C: 15.2 °C and 6.8 °C, and are plotted in Fig. 5. Again, the curves drawn were fitted to Eq. (2) by the method of least-squares, and have the following rate constants: 15.2 °C, 0.0877±0.0016 sec^{-1}; 6.8 °C, 0.0300± 0.0015 sec^{-1}. The curve at 25 °C ($k = 0.175$ sec^{-1}) is redrawn from Fig. 3*B* for comparison. From these results, lowered temperature reveals a Q_{10} between 2 and 3 for ATP decay in *Neurospora.*

Since it was not possible to manipulate the temperature for the voltage experiments with sufficient precision to duplicate the temperatures of the

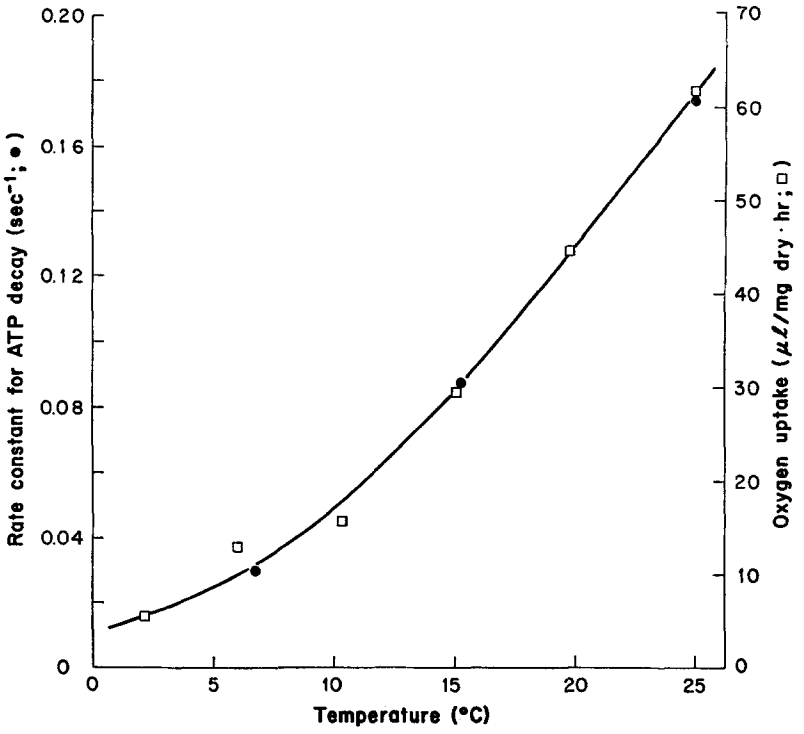

Fig. 6. Comparison of ATP decay and oxygen consumption as functions of temperature. Rate constants for ATP decay are taken from the curves in Figs. 3*B* and 5. Rates of oxygen consumption were determined with a Clarke-type electrode on cells suspended in solution F. Plotted values represent averages for two to five independent trials; average SEM's: 2.4 μliter/mg dry weight × hr. The following are interpolated rate constants to be compared with the voltage experiments:

Temp (°C)	k (sec^{-1})
24	0.167
21.2	0.141
16.0	0.0933
6.5	0.0304

ATP experiments, interpolation of rate constants became necessary. To avoid the considerable labor of further ATP measurements, and yet assess the reliability of the temperature curve based on three points, we decided to examine oxygen consumption by *Neurospora* at different temperatures. Respiration, if tightly coupled to ATP synthesis, should have the same overall temperature coefficient as the initial rate of ATP decay, since the uninhibited steady-state level of ATP is little affected by temperature. Oxygen consumption was measured on small volumes of cell suspension

Table 3. Parameter estimates for fitting Eq. (3) to membrane depolarization by cyanide and carbon monoxide

Temp (°C)	Rate const. constrained?	k (sec^{-1})	$1/k$ (sec)	A_1 (mV)	A_2 (mV)	Fitted interval (sec)	Points included	Σd^2
24	No	0.167 ± 0.005	5.99	47.4 ± 0.6	192.9 ± 4.9	5–30	11	6.8
	Yes	0.167	5.99	47.4 ± 0.6	192.9 ± 4.9			6.8
21.2	No	0.140 ± 0.007	7.15	26.6 ± 1.5	182.1 ± 5.3	5–26	15	33.1
	Yes	0.141	7.11	26.8 ± 1.5	182.6 ± 5.4			33.2
16.0	No	0.0735 ± 0.0015	13.6	26.3 ± 0.7	159.8 ± 1.8	6–54	29	31
	Yes	0.0933	10.7	32.2 ± 1.3	179.5 ± 6.4			220
6.5	No	0.0328 ± 0.0010	30.5	58.0 ± 0.7	117.1 ± 1.9	18–102	25	15
	Yes	0.0304	32.9	56.2 ± 0.9	113.6 ± 1.9			19
24 (CO)	No	0.135 ± 0.007	7.41	100.0 ± 1.3	162.3 ± 14.9	6–31	11	9
	Yes	0.167	5.99	97.1 ± 0.9	136.2 ± 5.6			32

The voltage plots are those of Figs. 4 and 7; ATP plots, Figs. 3*B*, 5, 6.

with a Clarke-type oxygen electrode, as described previously [45]. A joint plot of the observed rates of oxygen consumption and the computed rate constants for ATP decay, both plotted against time, is shown in Fig. 6. The two sets of data superimpose very easily, with a scaling factor of 348 μliter sec/mg dry wt × hr.

It is possible to calculate an apparent P/O ratio for intact cells from this scaling factor in the following manner. The scaling factor, on elimination of the time dimensions and conversion of dry weight to cell water, becomes 1.70 mmoles O_2/kg cell water. From Eq. (2) and Fig. 3*B*, the amount of ATP broken down in the presence of inhibitor is 2.36 mmoles/kg cell water, which would give a P/O ratio of $2.36/(2 \times 1.70) = 0.69$. However, previous studies [41] indicated that the total store of high-energy phosphate dissipated at the onset of respiratory inhibition is 8 to 9 mmoles/kg cell water, the additional amount normally being present as other nucleoside di- and triphosphates. If all of the phosphate split were to funnel through ATP, the actual unidirectional rate constant for ATP splitting could be 3.5-fold greater than the observed value for net breakdown. This would change the scaling factor in Fig. 6 to 0.49 mmoles O_2/kg cell water, and would give a P/O ratio of 2.4, which is within the range of values (2.0 to 3.0) to be expected for the *Neurospora* respiratory chain.

From the smooth curve in Fig. 6 rate constants for ATP decay at the onset of cyanide inhibition can be estimated for any desired temperature, in the range 3 to 25 °C. The appropriate values for comparison with voltage experiments are listed in the legend to Fig. 6 and also in Table 3 (third column).

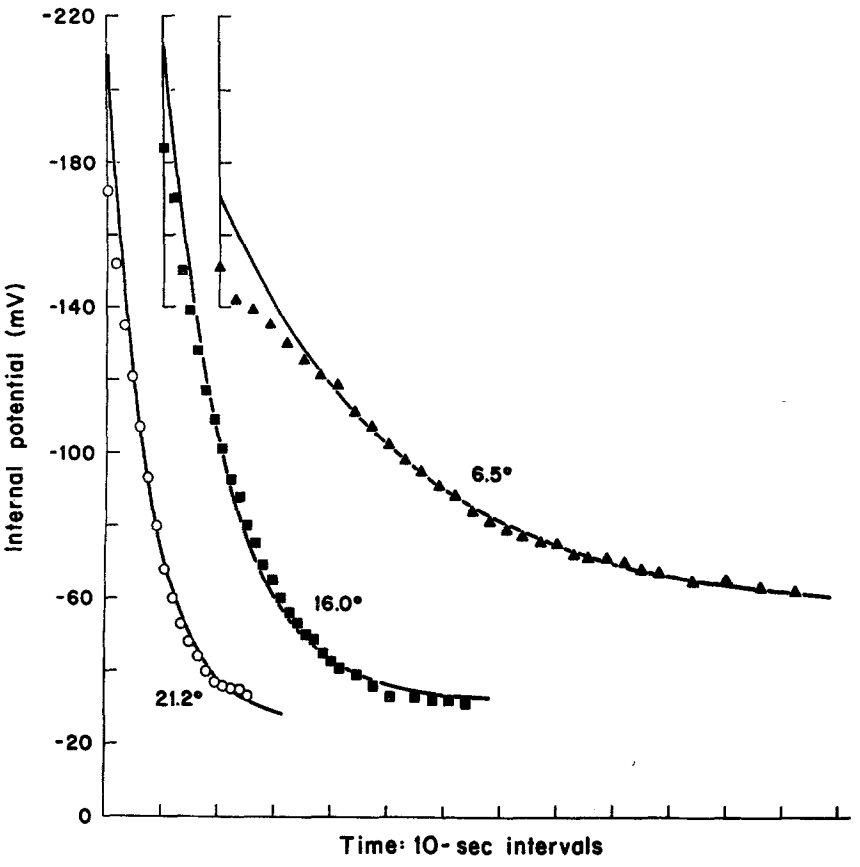

Fig. 7. Temperature effect on the time course of voltage decay with cyanide inhibition. All points plotted represent time-averaged values read from eight records for independent hyphae. Average SEM for all points is 7.6 per cent of the mean. Hyphae preincubated in solution D at the appropriate temperature for at least 30 min before rapid substitution with solution G. Average temperatures in the presence of cyanide: 21.2 ± 0.4 °C, 16.0 ± 0.2 °C, or 6.5 ± 0.1 °C. The curves were fitted to a single decaying exponential function [text Eq. (3)] using the rate constants determined from Fig. 6: 0.141 sec^{-1} at 21.2 °C, 0.0933 sec^{-1} at 16 °C, and 0.0304 sec^{-1} at 6.5 °C. The corresponding parameters A_1 and A_2 are listed in Table 3. Fits excluded the initial points in all three plots, as indicated also in Table 3

These new rate constants can be used, in the manner already employed at 24 °C (*see* Fig. 4), to fit simple exponential curves to the data on membrane potential at the respective temperatures. The results are shown in Fig. 7. Once again two phases are apparent in the process of depolarization: an initial phase of several seconds duration in which membrane potential falls slowly relative to ATP, and a prolonged phase in which the two functions change in almost exact parallel.

The quality of the fit is conditioned, of course, by the fact that there are still two adjustable parameters, A_1 and A_2, in Eq. (3) once the rate constant k has been fixed. To judge whether the fits, particularly that for 16 °C, differ significantly from the actual voltage data, it is useful to compute the least-squares curve which fits Eq. (3) to the voltage data without constraining the rate constants. A comparison of the appropriate fitted parameters for all four temperatures is given in Table 3. From a statistical point of view, it is clear that the constrained and unconstrained fits at 24 °C (with cyanide), at 21.2 °C and at 6.5 °C are essentially identical. But at 16 °C and 24 °C with carbon monoxide the constrained and unconstrained fits differ significantly from each other. The deviation, however, should not be regarded as lying outside the range of systematic error in the experiments. Two likely sources of error are inadequate temperature measurement, and physiological adaptation to respiratory blockade, which is a highly variable phenomenon [41].

The Initial Phase of Depolarization: V_m vs. ATP

In none of the measurements discussed above does the close parallel between the decay of ATP and the decline of membrane potential become evident earlier than several seconds after the onset of cyanide inhibition. In fact for all five cases plotted in Figs. 4 and 7, 30 to 50 per cent of the total ATP loss occurs before the voltage curves drop in parallel. Evidently, plots of the resting membrane potential directly against ATP concentration must show a tendency toward voltage "saturation" at the higher ATP concentrations, which correspond to the earlier times. The actual behavior of three such plots, for 24, 16 and 6.5 °C is shown in Fig. 8*A* (lower curve) and Fig. 8*B*. The general validity of the plots is supported by the fact that a curve of similar shape (upper curve, Fig. 8*A*) was obtained when the minimal membrane potential was plotted against the minimal ATP concentration, observed at a series of cyanide concentrations between 10^{-6} and 10^{-2} M.

Such data are readily fitted by a rectangular hyperbola, modified slightly from the Michaelis equation:

$$V_m = V_0 + \frac{V_{pm}[\mathrm{ATP}]_i}{K_{1/2} + [\mathrm{ATP}]_i}, \tag{5}$$

in which V_0 represents the membrane potential in the absence of electrogenic pumping; and V_{pm} represents the apparent maximal added voltage developed by the pump. Table 4 lists the three fitted parameters for the four cases plotted in Fig. 8. Since there is no *a priori* way to predict how temperature should affect enzyme kinetic parameters, the values listed in Table 4 must be taken simply as empirical results.

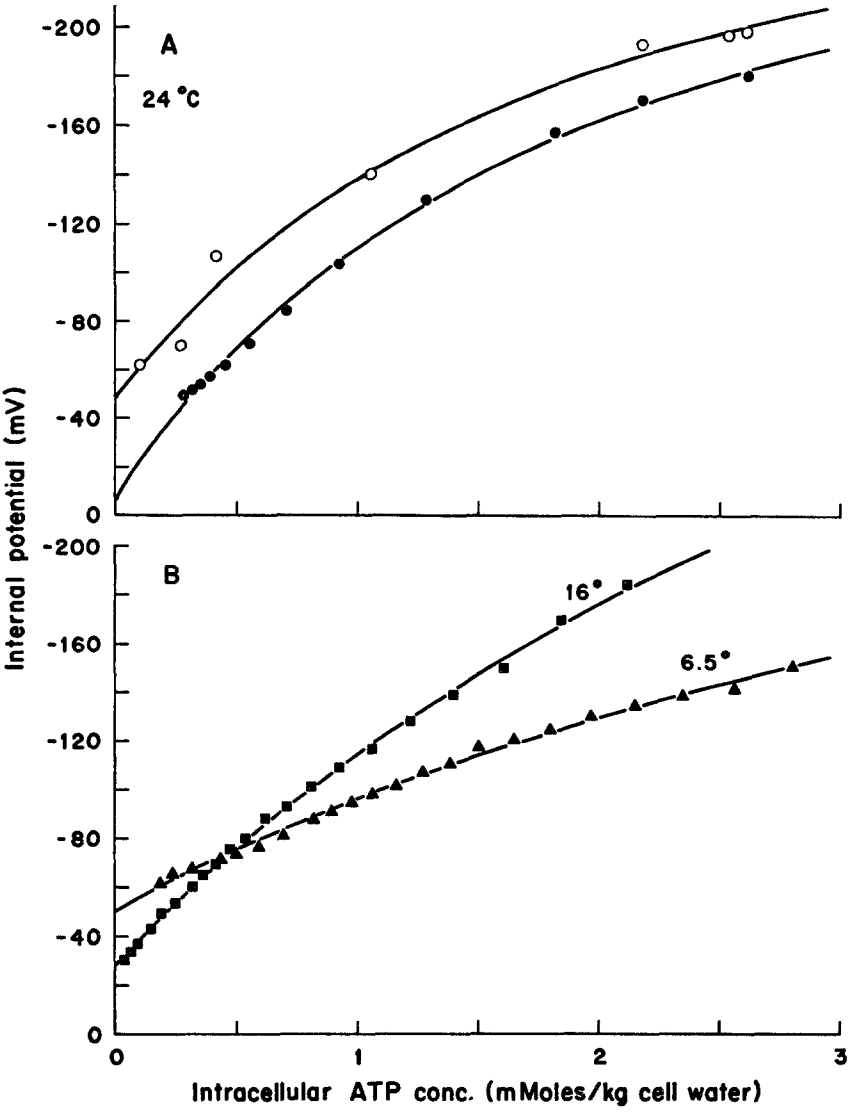

Fig. 8. Membrane potential as a function of the apparent intracellular ATP concentration. *Part A:* 24 °C. Points plotted along the upper curve represent average values for three determinations made 30 sec after the introduction of (neutralized) KCN at the following molar concentrations: 0, 10^{-6}, 10^{-5}, 3×10^{-5}, 10^{-4}, 10^{-3}, and 9×10^{-3}, read right to left on the plot. ATP and voltage measured in separate, parallel experiments. Average SEM's for voltage: 5.5 mV; for ATP: 0.13 mM. Cells and hyphae maintained in solution D until addition of cyanide at zero time. Points plotted in the lower curve represent interpolated values from the (dashed curve) voltage plot of Fig. 4*A* and, with the rate constant adjusted to 24 °C, the ATP curve of Fig. 3*B*. Times of interpolation (sec): 0, 1.25, 2.5, 2.5-sec intervals to 22.5, 30. *Part B:* lower temperatures. Points obtained in the manner of the lower curve of Part *A*, from the plots of Fig. 7 (voltage) and the fitted curves of Fig. 5 (ATP), again with the rate constants adjusted to the corresponding temperatures of the voltage experiments. Times of interpolation as follows, for 16 °C (sec): 0, 1.5-sec intervals to 21, 3-sec intervals to 30, 36, 42, 48, 54; for 6.5 °C (sec): 3-sec intervals to 42, 6-sec intervals to 66, 78, 90, 102. The curves drawn were fitted by least-squares to the sum of a constant term plus a rectangular hyperbola [text Eq. (5)], and the resultant parameters are listed in Table 4

Table 4. Parameters of the plots of voltage versus ATP concentration in *Neurospora*

Temp (°C)	V_0 (mV)	V_{pm} (mV)	$K_{1/2}$ (mM)
24 (DR)	48.4±5.1	268.9±22.4	2.00±0.43
24	7.0±6.6	310.7±23.9	2.00±0.43
16	28.6±1.0	497.9±40.8	4.76±0.55
6.5	50.4±0.5	299.9±32.1	5.53±0.92

Parameter estimates obtained by fitting Eq. (5) to the plots in Fig. 8. The first line represents the dose-response curve obtained at 24 °C, and the other three represent data from ATP and voltage transients. The two curves at 24 °C were fitted jointly, with $K_{1/2}$ held in common.

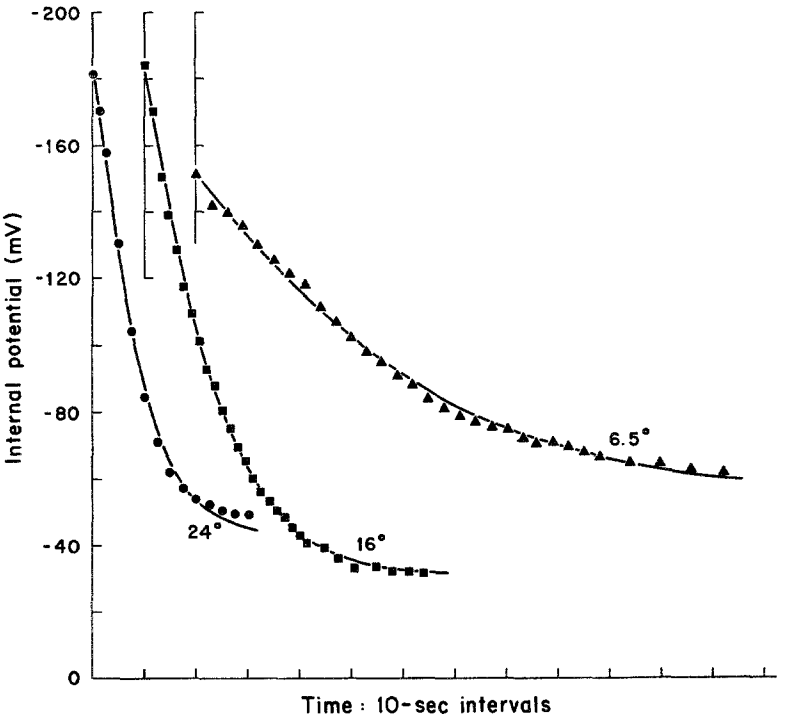

Fig. 9. Time courses of voltage decay produced by cyanide, fitted by the Michaelis equation. Data replotted from Figs. 4*A* and 7, and curves calculated from text Eq. (5), with $[ATP]_i$ substituted by Eq. (2); parameters listed in Tables 3 and 4

Fig. 9 shows replots of the data for voltage versus time (Figs. 4*A* and 7) with the curves calculated by substituting Eq. (2) into Eq. (5) and using the appropriate parameters from Tables 3 and 4. Over the time intervals for which simple exponential fits of voltage *versus* time were previously obtained (*see* Table 3), the modified Michaelis equation gives a better fit at 16 °C and a less satisfactory fit at 24 °C and 6.5 °C than did the exponential equation (constrained). (Corresponding sums of squared differences (Σd^2)

are 89, 55, and 88 at 24, 16 and 6.5 °C, respectively, in Fig. 9; compared with 6.8, 220, and 19 in Table 3.) The Michaelis curve, however, clearly describes the initial points at all three temperatures, which the simple exponential, constrained to the rate for ATP, cannot do.

Release from Respiratory Inhibition

Metabolic recovery following quick removal of a respiratory inhibitor displays more complicated kinetics than are seen at the onset of inhibition, even when the delays inherent in removing an inhibitor from bulk solution are minimized. It has already been shown, for example, that intracellular ATP recovers approximately linearly for 10 sec (25 °C) when a 1-mM solution of sodium azide is removed [41]. (Azide was used in this experiment because anoxia could not be maintained under the conditions of the ATP experiments, and because azide, but not cyanide, has a low enough pK so that "pH trapping" [41] could be used to speed washout of the inhibitor.) Thereafter, $[ATP]_i$ passes through a maximum and subsides toward a steady level. The initial linear phase, overshoot, and slow stabilization were all seen also with pyridine nucleotide oxidation and with the membrane potential (Fig. 10), so that the recovery data, unlike the data for the onset of inhibition, do not by themselves rule out a possible direct dependence of voltage upon electron transfer.

The empirical relationship between the membrane potential and $[ATP]_i$, defined by the curves of Fig. 10*B* and 10*C*, is conspicuously sigmoid, as shown in Fig. 11. Despite the difference in shape between this curve and the ones in Fig. 8, inspection of the curve for recovery suggests that both the maximal pump voltage and the ATP concentration giving half the maximal voltage lie in the neighborhood of the values ($V_{pm} = 311$ mV; $K_{1/2} = 2.0$ mM) obtained for the onset of respiratory inhibition. The maximal slope of the curve in Fig. 11 occurs at about 1 mM ATP, and is equal to 124 mV/mM. The corresponding slope from the Michaelis curve (lower) of Fig. 8*A* is 69 mV/mM. The larger slope observed during recovery is thought to be related to increased membrane resistance, and will be considered in detail in the Discussion.

Another estimate of the relationship between voltage and intracellular ATP during release from respiratory inhibition was obtained in a fortuitous experiment with carbon monoxide. In the process of setting up the experiment of Fig. 4*B*, some preliminary tests were run on the electronic shutter which controlled the light flashes. During these tests the record shown in Fig. 12*A* was traced out. When kept dark, in buffer saturated with 97% CO/3% O_2, the hypha maintained a resting membrane potential of −90 mV;

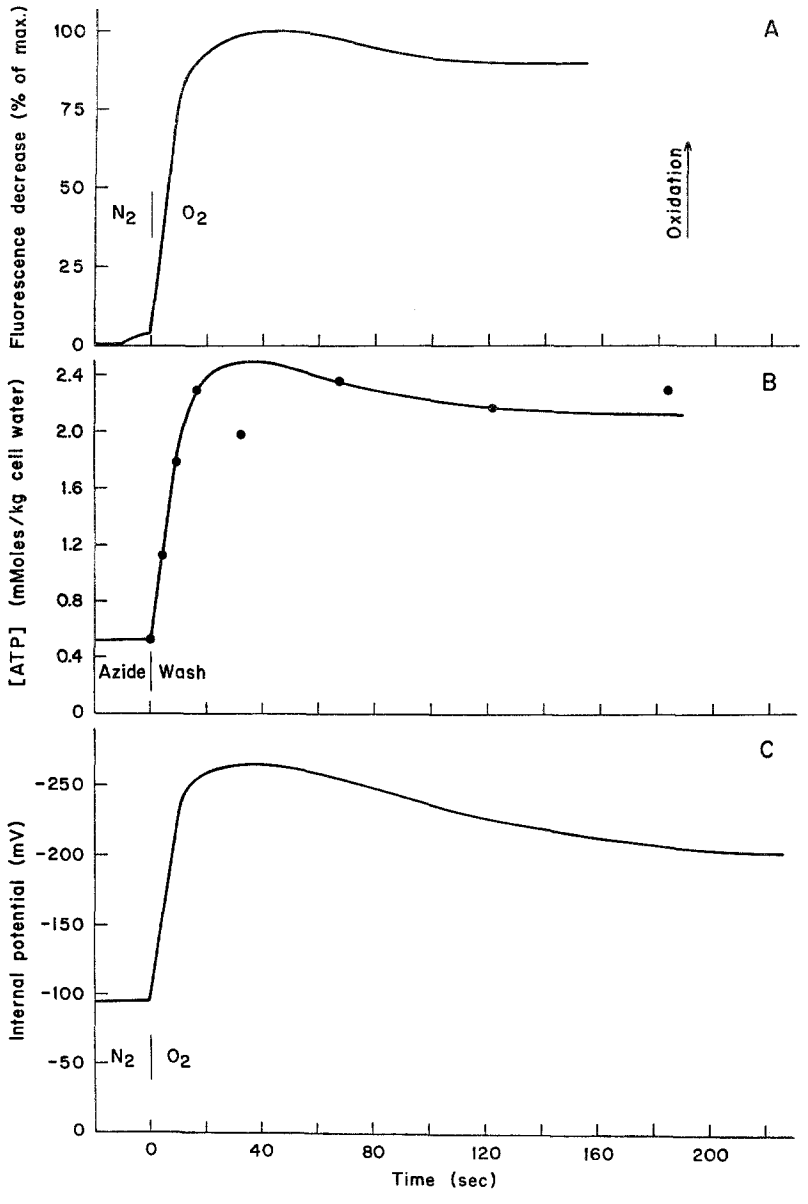

Fig. 10. Time course of release from respiratory inhibition. *Part A:* Pyridine nucleotide fluorescence. Cells suspended at a density of 3.5 mg dry weight/ml in solution B saturated with nitrogen. Oxygen bubbling begun at zero time. Fluorescence trace replotted from a record obtained at the Johnson Foundation, University of Pennsylvania (*see* Methods). *Part B:* ATP data redrawn from Slayman [41], Fig. 8. Average SEM's 0.19 mM. *Part C:* Voltage data obtained from hypha maintained in nitrogen-saturated solution A, in the presence of a dense suspension of shaking-culture cells (3.5 mg dry weight/ml) to insure anoxia. Chamber flushed rapidly with cell-free, oxygen-saturated solution at zero time.

Voltage trace redrawn in order to be scaled with ATP and fluorescence data

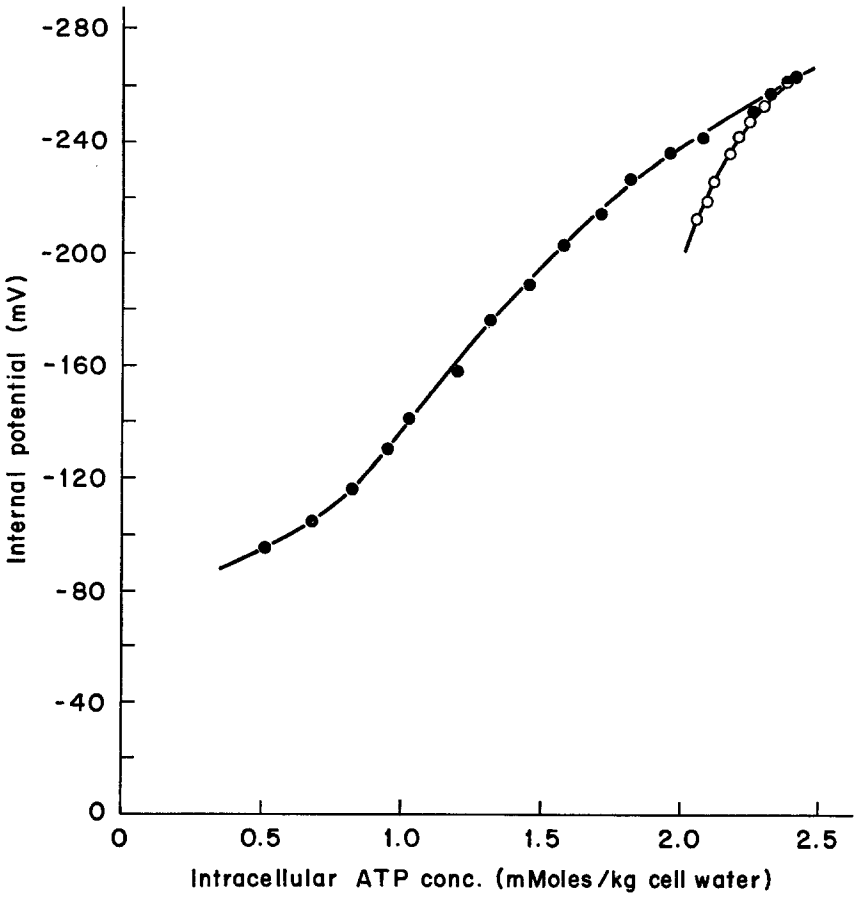

Fig. 11. Membrane potential as a function of apparent intracellular ATP during recovery from respiratory blockade. Points were obtained by reading along the curves of Figs. 10*B* and 10*C* at the following times (sec): 0, 1-sec intervals to 12, 16, 20, 6-sec intervals to 44, 52, 60, 10-sec intervals to 100. Filled circles (•) obtained along the rising limb of the voltage curve; open circles (o), along the falling limb. The curves are drawn by eye. The maximum slope on the curve of rising voltage is 124 mV/mM (occurring at 1 mM ATP)

with a sustained saturating light the voltage stabilized at −167 mV; and with brief light flashes of varying length, voltage transients of varying amplitude were generated. The corresponding plot of voltage amplitude versus flash duration is shown in Fig. 12*B*, and is fitted by a straight line constrained to pass through the origin. The slope of that line, 12.6 mV/sec, can be used to calculate the slope of voltage versus $[ATP]_i$, if ATP recovery is assumed to occur as in Fig. 10*B*: initial slope 0.131 mM/sec. The resulting value, 96 mV/mM should be compared with the slope of the lower curve in Fig. 8*A* at 114.9 mV, which is 66 mV/mM. Again, the difference may be accounted for by a change in membrane resistance.

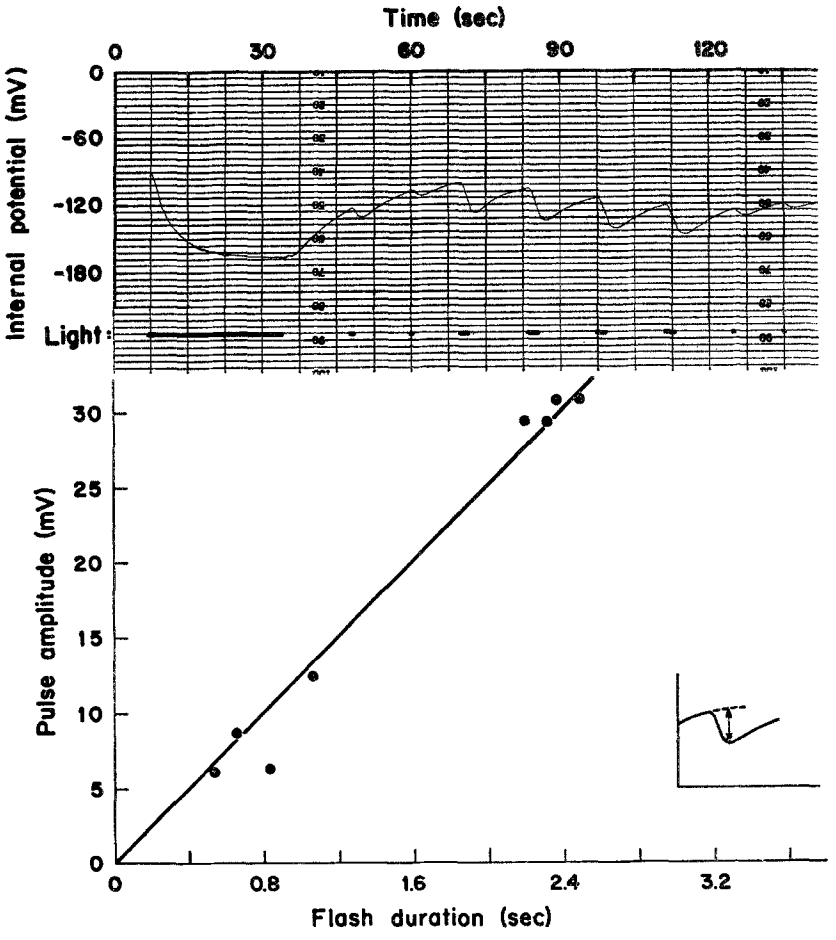

Fig. 12. Recovery of membrane potential during pulsed release from carbon monoxide inhibition. *Upper trace:* voltage record. *Lower graph:* plot of pulse amplitude (measured as shown in the inset) versus duration of a saturating light flash (*see* black bars at bottom of trace). The straight line is fitted by least-squares, constrained to pass through the origin. Slope: 12.6 ± 0.4 mV/sec

Effects of other Inhibitors

The major reason for using cyanide as the principal inhibitor in these experiments is that, at least for low concentrations, its action in blocking respiration at cytochrome a_3 is specific; it yields simple kinetics for both ATP and voltage. A variety of other inhibitors have given more complicated kinetics for changes of ATP and/or membrane potential. Therefore, the resultant voltage/ATP comparison is more difficult to interpret, though certainly not to an extent which vitiates the conclusions drawn from studies with cyanide. Table 5 lists the major features of ATP and voltage responses to six different inhibitors.

Table 5. Summary of effects of various inhibitors on ATP and membrane potential

Inhibitor	Conc. (M)	Primary effect	Change in ATP	Calc. change V_m	Meas. change V_m
Cycloheximide	3.5×10^{-4}	Blocks protein synthesis	Linear decrease to 62% of control in 10 min	Depol. 37 mV	Depolarization by 25 mV in 7 min; then faster
0 Ca^{++} at pH 8.2	—	?	Linear decrease for 5 min at 9.5%/min. Stable at 50%	Depol. 8 mV/min	Linear depol. at 8 mV/min for 25 min
11-Deoxycorticosterone (DOC)	1×10^{-3}	?	Steady-state loss to 60%	Depol. 42 mV	2-phase depol. by 116 mV in 1.5 min
2-Deoxyglucose (2-DOG)	6.1×10^{-2}	Blocks phosphohexose isomerase	Exponential decr. to 16% in 5 min	Depol. 115 mV	2-phase depol. by 55 mV in 10 min. R_L increase by 50%
Carbonyl cyanide *m*-chlorophenyl hydrazone (CCCP)	1×10^{-5}	Uncouples oxid. phosphorylation	Exponential decr. to 36%. Time constant = ca. 5.5 sec	Depol. 77 mV	2-phase depol. by 67 mV in 100 sec, followed by slow decline, and increase of R_M
2,4-Dinitrophenol (DNP)	1×10^{-3}	Uncouples oxid. phosphorylation	Exponential decr. to 20%. Time constant = 7.8 sec	Depol. 67 mV at 11 sec. Depol. 104 mV, end	Pause and/or sharp drop by as much as 60 mV, lasting 8–11 sec, followed by exp. decline with time const. $\simeq$ 7.8 sec

Changes of ATP with cycloheximide and with 0-Ca^{++} at pH 8.2 are described from Slayman [41], Fig. 3. Eq. (5), with the parameters listed in Table 4 for 24 °C, was used to calculate the voltage changes expected (column 5) for the given percentage decrease in ATP. Each control ATP concentration (100%) was calculated first, with the measured control voltage entered for V_m.

For the first two inhibitors listed, cycloheximide and zero calcium at high pH, the initial rates of decay of ATP and membrane potential are commensurate, given the relationship defined by Eq. (5), though at longer times the agreement is less good. For the third inhibitor, deoxycorticosterone (DOC), both ATP and membrane potential reach minima quickly, but the amount of depolarization is about threefold that calculated from the change in ATP. DOC is the only inhibitor found for which the voltage change is *greater* than expected, and the result is consistent with the suggestion of Lester, Stone, and Hechter [21] that DOC acts directly on transport systems. For the other three agents the time courses of voltage change are more complex than the time courses for ATP change. With 2-deoxyglucose (2-DOG), depolarization appears to be retarded by a factor of 2 to 3 in comparison with ATP changes, which might result from larger stores of endogenous carbohydrates [59] and perhaps phosphorylated intermediates in the mature hyphae used for the electrical experiments. The uncoupling agent, carbonyl cyanide *m*-chlorophenyl hydrazone (CCCP), depolarizes slowly and in the three distinct phases or "steps" of about 10 mV, 50 to 80 mV, and another 20 to 60 mV. The steps and the slowness of response are eliminated by going to 10^{-4} M CCCP – a concentration which is far supramaximal for effects on ATP – suggesting that the uncoupler has less free access to the mitochondria in the mature hyphae than it does in the smaller cells from liquid shaking cultures. This conceivably could result from more efficient screening by the cell wall, or more efficient breakdown of the substance within the cytoplasm, but no specific evidence is available. Finally the more common uncoupling agent, 2,4-dinitrophenol (DNP), has a two-step effect on voltage. The first is a small, rapid drop in potential which is accompanied by an approximately twofold drop in membrane resistance[1]; the second is an exponential depolarization which follows the time course of ATP. It is likely that results with both uncouplers are complicated by direct action of DNP or CCCP on the permeability of the plasma membrane [16].

Discussion

Is the Electrogenic Pump an ATPase?

From the nature of the experiments discussed above, it is not possible to state unequivocally that ATP is the immediate energy source for the electrogenic pump in *Neurospora*. That conclusion would require either *in vitro* study of the transport system or controlled perfusion of intact hyphae; and neither of these experiments is feasible at the present time.

1 D. Gradmann and C. L. Slayman *(manuscript in preparation)*.

Substantial quantities of non-adenine nucleoside di- and triphosphates exist in *Neurospora*: in particular, 0.4 mM GTP and CTP [41], and probably equal amounts of TTP and UTP. No detailed time-course studies have been carried out on these other nucleotides, but it is conceivable that one of them mediates between ATP and the pump.

To obtain some quantitative appreciation of this possibility, a two-compartment model was developed in which the membrane potential was assumed to be directly proportional to the concentration of an intermediate XP which was derived from ATP; the model was simplified by assuming that the unidirectional rate constants for ATP/XP interconversion were equal and that the rate constants for breakdown of ATP (general) and XP (pump) were equal. The solutions to the resulting differential equations gave ATP as the sum of two exponentials, plus a constant term, and gave V_m proportional to the difference of the same two exponentials plus another constant term. The expressions were then fitted jointly to the data for ATP and V_m (as functions of time), yielding estimates for the rate constants and for size of XP. At 24 °C, for example, the rate constant for breakdown of ATP and XP was 0.147 sec^{-1}, about 90% of that computed from the single exponential fit (Fig. 3*B*); the rate constant for interconversion of ATP and XP was 0.053 sec^{-1}, about 35% of that for breakdown; and the normal steady-state concentration of XP was 0.64 mM, about 25% of $[ATP]_i$. However, at all temperatures the voltage fits were several-fold less good, as judged by the sum of squared deviations, than for the Michaelis function fitted in Fig. 9.

One result which may seem disconcerting is the large value of $K_{1/2}$ for ATP (Table 4): 2 mM at 24 °C, and 4.8 to 5.5 mM at the lower temperatures. While a time-dependent decrease in membrane leakage resistance could give a falsely high estimate of $K_{1/2}$ in the temperature shift experiments (*see below*), no such argument can be invoked to account for a $K_{1/2}$ of 2 mM at the normal temperature. Tabulation of parameters for established ATPases and ATP-linked phosphotransferases, however, has indicated that 2 mM, although a high value of $K_{1/2}$, is not inordinately so. Individual enzymes along the glycolytic pathway, on the paths of amino acid and nucleotide metabolism, and among transport-related ATPases have $K_{1/2}$ values for ATP lying between 1 and 8 mM [3, 7, 15, 17, 34, 36]. Most importantly, ATPases separated from energy conserving membranes *generally* display $K_{1/2}$'s of 0.3 mM or higher. Enzyme assayed in detergent-extracted mitochondria shows $K_{1/2}$ values of 0.45 to 1.4 mM, depending on calcium and magnesium concentrations [53]; that from partially purified membranes of *Bacillus megaterium* or *Bacillus stearothermophilus* has a $K_{1/2}$ of 3 mM [25, 56]. Most importantly the ATPase released (by low-Mg washing) from ghosts of *Streptococcus faecalis* has an ATP-$K_{1/2}$ of 2 mM, which is elevated to 8 mM in the presence of 2.5 mM ADP [1]. Thus, to the extent that the enzyme underlying the electrogenic pump in the *Neurospora* membrane is analogous to the ATPase of energy-conserving membranes, its $K_{1/2}$ for ATP would be expected to be in the neighborhood of 1 mM, and

Table 6. Computation of the concentration term for the free energy of hydrolysis of ATP

Time (sec)	$[ATP]_i$ (mM)	$[ADP]_i$ (mM)	$[P_i]$ (mM)	$K=\frac{[ADP]_i \cdot [P_i]}{[ATP]_i}$	$RT\ln K$ (kcal)
0 (add CN^-)	2.64	0.78	10	2.96×10^{-3}	−3.45
30 (minimum)	0.53	1.17	~15	33.8×10^{-3}	−2.00
180	0.72	1.09	~15	22.7×10^{-3}	−2.24
0 (wash Az^-)	0.52	0.96	~18	33.2×10^{-3}	−2.02
30 (peak)	2.50	0.41	~13	2.13×10^{-3}	−3.64
180	2.14	0.55	~13	3.34×10^{-3}	−3.37

Nucleotide values are taken from Slayman [41], Figs. 6 and 8. The control value of inorganic phosphate was calculated from Harold [13], and the other values were estimated from changes in total nucleotide levels [41].

might also be modulated by ADP (present in *Neurospora* at 0.4 to 1.5 mM [41]) or perhaps by inorganic phosphate (present at levels of 10 to 20 mM [13]).

From a comparison of the measured membrane potential V_m and the free energy available from the hydrolysis of ATP, the electrogenic pump would appear, at least marginally, able to move (H^+) ions on a two-to-one basis for ATP split. By linear interpolation from the tabulated results of Phillips *et al.*, (Table IV [28]), it is possible to estimate a standard empirical free energy (ΔG_{obs}) for the hydrolysis of ATP equal to −8.54 kcal/mole, with the following parameters specified: ionic strength = 0.2, intracellular pH = 6.46 [43], and magnesium concentration = 16 mM [54]. The total free energy for hydrolysis of ATP can be estimated from ΔG_{obs} by adding the term for concentrations:

$$\Delta G_T = \Delta G_{obs} + RT\ln\frac{[ADP]_i[P_i]}{[ATP]_i}. \tag{6}$$

The pertinent data for calculation are listed in Table 6. Assuming the reactants to be essentially homogenously distributed, the free energy available to the electrogenic pump at the instant respiration is blocked is $-(8.54+3.45) = -11.99$ kcal/mole, which corresponds to 520 mV. At the end of the rapid phase of depolarization (30 sec), and again after a prolonged period of inhibition (30 min in azide), the available energy is approximately −10.54 kcal/mole = 457 mV. And at the peak of recovery following washout of azide, the available energy is −12.18 kcal/mole = 528 mV. Rough average membrane potentials measured at the corresponding times are (absolute values) 190 mV, 50 mV, and 250 mV, respectively. A two-charge process generating 250 mV would require free energy equivalent to 500 mV, equal −within the limits of precision of the overall calculation −to the maximal free energy available from ATP hydrolysis. The simplest stoichiometry to envision, therefore, is 2:1, a result which is in keeping with the presumed

stoichiometry for ATP synthesis in mitochondria. The fact that $(V_0 + V_{pm}) \times 2$ can be considerably greater than the energy released by ATP splitting (Table 4) is not inconsistent with the above argument, since V_{pm} is determined by extrapolation of $[ATP]_i$ to high values, where $[ADP]_i$ would be low and the concentration term in Eq. (6) could be very large.

From a stoichiometry of 2:1, the ATP turnover required to sustain the membrane potential in *Neurospora* can also be calculated. 200 mV, maintained across a leakage resistance (R_L, *see below*) of 10 kohms cm^2 [39] requires a current of approximately 20 μA/cm^2 = 200 pmoles/cm^2 × sec. Hyphae used in the electrical experiments average 15 to 20 μ in diameter; the ratio of cell water/dry weight = 2.54 [46]; and an average specific density of 1.0 is assumed. Then the surface area corresponding to a kilogram of cell water is 3.19×10^6 cm^2; and 200 pmoles/cm^2 × sec = 0.64 mmoles/kg cell water × sec, or 38 mmoles/kg cell water × min. On division by 2, this corresponds to 19 mmoles of ATP/kg cell water × min. The average rate of ATP synthesis from oxidative metabolism was previously calculated at 70 mmoles/kg cell water × min [41], so that the electrogenic pump would drain off 27% of the total metabolic supply of high-energy phosphate. A simple way in which to reconcile such a large energy drain with the apparent fact that *Neurospora* is not a specialized transport tissue is to suppose that the resultant electrical gradient is used to drive the transport of other substances into *Neurospora* via cotransport carriers [44], in the manner already indicated for sugar transport in bacteria [57].

Relation to the Membrane Equivalent Circuit

For the present discussion the clearest equivalent circuit to use for the *Neurospora* membrane is that shown in Fig. 13, in which the electrogenic pump is represented as a current source (i_p) and the ion diffusion regimes (leaks) are represented as a voltage source (E_L) in series with a resistance (R_L). From this circuit, the total membrane potential (V_m) is

$$V_m = E_L + i_p R_L, \tag{7}$$

in which the terms can be directly equated with the corresponding terms of Eq. (5). Setting the Michaelis term equal to $i_p R_L$, dividing through by R_L, and then letting $V_{pm}/R_L = i_{pm}$, gives

$$i_p = \frac{i_{pm} \cdot [ATP]_i}{K_{1/2} + [ATP]_i}. \tag{8}$$

Eq. (5) can now be written

$$V_m = V_0 + R_L \frac{i_{pm} \cdot [ATP]_i}{K_{1/2} + [ATP]_i}, \tag{9}$$

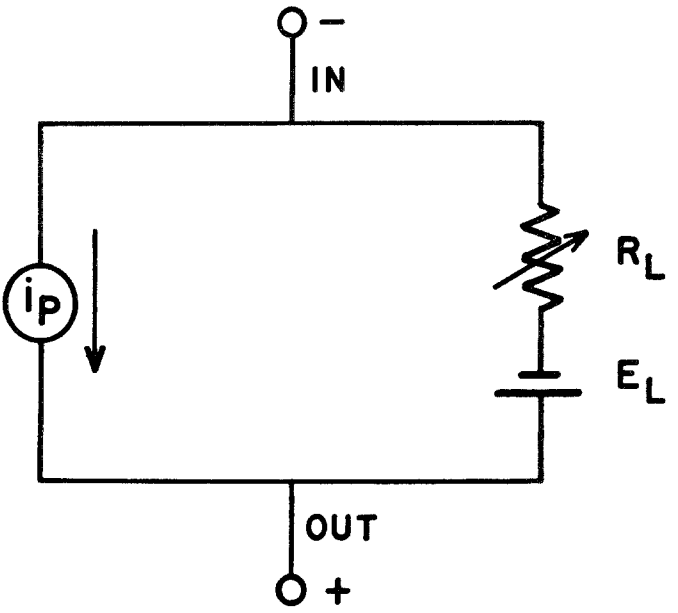

Fig. 13. An equivalent circuit for the *Neurospora* membrane. i_p represents the electrogenic pump as an ideal current source. Ion diffusion pathways (leaks) are represented as a net EMF (E_L) and variable resistance (R_L) in series

in which the Michaelis term is a real pump velocity, and R_L is a scaling factor which relates the pump velocity to the actual membrane potential.

If the fundamental relationship between pump current and ATP levels is assumed to be the saturation (Michaelis) curve given by Eq. (8), then a number of features of the actual curves relating voltage to ATP remain to be accounted for in the properties of R_L: (a) The slight inflection at 0.4 mM in the *data* for V_m versus $[ATP]_i$ during the onset of cyanide inhibition (Fig. 8*A*, lower plot); (b) The conspicuous sigmoid character of the plot of V_m versus $[ATP]_i$ during release of inhibition (Fig. 11); (c) The steep slope relationship between voltage and ATP with release of inhibition (*see* discussion of Figs. 11, 12*B*); (d) The very large value of V_{pm} at 16 °C (Table 4); and (e) The large values of $K_{1/2}$ at both 16 °C and 6.5 °C (Table 4). Although detailed resistance measurements have not been carried out in conjunction with the ATP experiments, it is nervertheless useful to point out the properties of R_L which would be required to account for the above results, and to indicate the extent to which existing resistance data are qualitatively consistent.

The inflection at 0.4 mM in Fig. 8*A* (lower curve) could result from an increase of no more than 10% in the value of R_L at the end of the voltage transient. A small (30 to 70%) increase in total membrane resistance has

been observed during the onset of respiratory inhibition[1] but modeling analysis indicates that change to be associated mainly with the internal resistance of the pump (which does not behave in detail like an ideal current source). R_L appears to be constant, with an uncertainty of $\pm 10\%$, sufficient to allow the change required by the data of Fig. 8. The more conspicuous sigmoid curve seen during recovery cannot be accounted for by a simple monotonic change in R_L; but the steep slopes of voltage versus ATP inferred from both the postanoxic experiment (Fig. 11, 1 mM ATP) and the CO-recovery experiment (Fig. 12*B*) probably derive from a large (two- to threefold) increase in R_L which accompanies prolonged respiratory blockade and which reverses slowly during recovery[1]. In the postanoxic experiment 124 mV/mM is 1.80 × the slope in Fig. 8*A* at the same ATP concentration, and in the CO-recovery experiment 96 mV/mM is 1.45 × the slope in Fig. 8*A* at the same voltage. Therefore, 3 sec after reoxygenation R_L should be near 1.8 × its normal value; and the partial inhibition produced by sustained treatment with 97% CO/3% O_2 (dark) should be associated with a 1.45-fold increase of R_L. The large value of V_{pm}, 498 mV, calculated at 16 °C suggests that R_L is increased by 60% (1.6-fold), and temperature-dependent changes of this magnitude have been observed[1]. The lower value of V_{pm} at 6.5 °C probably reflects simply a reduced maximal velocity of the pump at low temperature. Elevated values of $K_{1/2}$ would result if, during the period of cyanide treatment, R_L relaxes somewhat following the initial temperature-dependent increase.

Once again it should be emphasized that in these experiments a comparison is being drawn between electrical measurements necessarily made on large, mature hyphae and chemical measurements made on small cells from shaking cultures. The validity of the comparison is strongly supported by the fact that specific control experiments gave essentially identical rate constants for the decay of ATP in the two cell types (see Methods). A major unresolved problem, however, in the magnitude of membrane potential in the small cells. The diameter of these cells is 2 to 3 μ, compared with 15 to 20 μ in the mature hyphae, so that the surface/volume ratio of the former is sevenfold greater. If the density of transport and leak sites is the same for the two kinds of membrane, the membrane potential in the small cells would necessarily be low; to maintain it near 200 mV would require $7 \times 19 =$ 133 mmoles of ATP/kg cell water × min, which would be 190% of the total ATP turnover. Thus, the value of V_{pm} [Eq. (5)] would be much smaller than the 311 mV calculated for mature hyphae, although V_0 and $K_{1/2}$ would not be affected. On the other hand, membrane potential in the small cells could be maintained at the same level as in the mature hyphae, if the density

of transport and leak sites were diminished in proportion to the increase of membrane area, i.e., kept constant in relation to cytoplasmic volume. Such a change in membrane properties raises interesting questions about physiologic control of membrane composition and assembly – a subject which has recently come under intense study in other microorganisms [9].

The authors are indebted to Mrs. Linda Shane and Mrs. Pamela Orchard for expert technical assistance, to Dr. William Miller for loan of an electronic shutter, and to Drs. Dietrich Gradmann, Carolyn Slayman, and Knox Chandler for much helpful discussion. The work was supported by Research Grants GM-12790 and GM-15858, by RCD Award GM-20164 (to C.L.D.) and by Postdoctoral Research Fellowship AM-16807 (to W.S.L.) from the National Institutes of Health.

References

1. Abrams, A. 1965. The release of bound adenosine triphosphatase from isolated bacterial membranes and the properties of the solubilized enzyme. *J. Biol. Chem.* **240**:3675
2. Adrian, R. H., Slayman, C. L. 1966. Membrane potential and conductance during transport of sodium, potassium, and rubidium in frog muscle. *J. Physiol.* **184**:970
3. Anderson, P. M., Wellner, V. P., Rosenthal, G. A., Meister, A. 1970. Carbonylphosphate synthetase (*Escherichia coli*). *In:* Methods in Enzymology. H. Tabor and C. W. Tabor, editors. Vol. XVII, p. 235: Metabolism of amino acids and amines, Part A. Academic Press, Inc., New York
4. Aubert, X., Chance, B., Keynes, R. D. 1964. Optical studies of biochemical events in the electric organ of *Electrophorus. Proc. Roy. Soc., B.* **160**:211
5. Brody, S. 1972. Regulation of pyridine nucleotide levels and ratios in *Neurospora crassa. J. Biol. Chem.* **247**:6013
6. Chance, B., Williams, G. R. 1955. Respiratory enzymes in oxidative phosphorylation. IV. The respiratory chain. *J. Biol. Chem.* **217**:429
7. Falcoz-Kelly, F., Cohen, G. N. 1970. Aspartokinase II and homoserine dehydrogenase II. *In:* Methods in Enzymology. H. Tabor and C. W. Tabor, editors. Vol. XVII, p. 699. Metabolism of amino acids and amines, Part A. Academic Press Inc., New York
8. Fein, H. 1966. Passing current through recording glass micropipette electrodes. *IEEE Trans. Bio-med. Eng.* **13**:211
9. Fox, C. F. 1972. Membrane assembly. *In:* Membrane Molecular Biology. C. F. Fox and A. Keith, editors. p. 345. Sinaur Associates, Stamford, Connecticut
10. Gibson, Q. H. 1963. Inhibitors of gas transport. *In:* Metabolic Inhibitors: A Comprehensive Treatise. R. M. Hochester and J. H. Quastel, editors. Vol. II, p. 539. Academic Press, Inc., New York
11. Gonzalez, C. F., Shamoo, Y. E., Brodsky, W. A. 1967. Electrical nature of active chloride transport across short-circuited turtle bladders. *Amer. J. Physiol.* **212**:641
12. Gradmann, D. 1970. Einfluß von Licht, Temperature und Außenmedium auf das elektrische Verhalten von *Acetabularia crenulata. Planta* **93**:323
13. Harold, F. M. 1962. Depletion and replenishment of the inorganic polyphosphate pools in *Neurospora crassa. J. Bacteriol.* **83**:1047
14. Harold, F. M. 1972. Conservation and transformation of energy by bacterial membranes. *Bact. Rev.* **36**:172

15. Hers, H. G. 1955. Fructokinase (ketokinase). *In:* Methods in Enzymology. S. P. Colowick and N. O. Kaplan, editors. Vol. I, p. 286. Academic Press Inc., New York
16. Hopfer, U., Lehninger, A. L., Thompson, T. E. 1968. Protonic conductance across lipid bilayer membranes induced by uncoupling agents for oxidative phosphorylation. *Proc. Nat. Acad. Sci.* **59**:484
17. Kasbekar, D. K., Durbin, R. P. 1965. An adenosine triphosphatase from frog gastric mucosa. *Biochim. Biophys. Acta* **105**:472
18. Kernan, R. P. 1970. Electrogenic or linked transport. *In:* Membranes and Ion Transport. E. E. Bittar, editor. Vol. I, p. 395. Wiley-Interscience, New York
19. Kitasato, H. 1968. The influence of H^+ on the membrane potential and ion fluxes of *Nitella*. *J. Gen. Physiol.* **52**:60
20. Lambowitz, A. M., Slayman, C. W., Slayman, C. L., Bonner, W. D. 1972. The electron transport components of wild type and Poky strains of *Neurospora crassa*. *J. Biol. Chem.* **247**:1536
21. Lester, G., Stone, D., Hechter, O. 1958. The effects of deoxycorticosterone and other steroids on *Neurospora crassa*. *Arch. Biochem. Biophys.* **75**:196
22. MacRobbie, E. A. C. 1970. The active transport of ions in plant cells. *Quart. Rev. Biophys.* **3**:251
23. Marmor, M. F. 1971. The independence of electrogenic sodium transport and membrane potential in a molluscan neurone. *J. Physiol.* **218**:599
24. Marquardt, D. W. 1963. An algorithm for least-squares estimation on non-linear parameters. *J. Soc. Ind. Appl. Math.* **11**:431
25. Marsh, C., Militzer, W. 1956. Thermal enzymes. VII: Further data on an adenosine triphosphatase. *Arch. Biochem. Biophys.* **60**:433
26. Mitchell, P. 1966. Chemiosmotic coupling in oxidative and photosynthetic phosphorylation. *Biol. Rev.* **41**:445
27. Mitchell, P. 1970. Reversible coupling between transport and chemical reactions. *In:* Membranes and Ion Transport. E. E. Bittar, editor. Vol. I, p. 192. Wiley-Interscience, New York
28. Phillips, R. C., George, P., Rutman, R. J. 1969. Thermodynamic data for the hydrolysis of adenosine triphosphate as a function of pH, Mg^{2+} ion concentration, and ionic strength. *J. Biol. Chem.* **241**:3330
29. Raven, J. A. 1968. Action spectra for photosynthesis and light-stimulated ion transport processes in *Hydrodictyon africanum*. *New Phytol.* **68**:45
30. Raven, J. A. 1968. Effects of inhibitors on photosynthesis and the active influxes of K and Cl in *Hydrodictyon africanum*. *New Phytol.* **68**:1089
31. Rehm, W. S. 1966. Electrogenic mechanism of the frog's gastric mucosa. *Ann. N.Y. Acad. Sci.* **137**:591
32. Rehm, W. S. 1972. Proton transport. *In:* Metabolic Pathways. VI. Metabolic Transport. L. E. Hokin, editor. p. 187. Academic Press Inc., New York
33. Ritchie, J. M. 1971. Electrogenic ion pumping in nervous tissue. *Curr. Top. Bioenerget.* **4**:327
34. Roon, R. J., Levenberg, B. 1970. ATP: Urea amidolyase (ADP) (Candida utilis). *In:* Methods in Enzymology. H. Tabor and C. W. Tabor, editors. Vol. XVII, p. 317. Metabolism of amino acids and amines, Part A. Academic Press Inc., New York
35. Saddler, H. D. W. 1970. The membrane potential of *Acetabularia mediterranea*. *J. Gen. Physiol.* **55**:802
36. Schoner, W., Beusch, R., Kramer, R. 1968. On the mechanism of Na^+- and K^+-stimulated hydrolysis of adenosine triphosphate. 2. Comparison of nucleotide specificities of Na^+- and K^+-activated ATPase and Na^+-dependent phosphorylation of cell membranes. *Europ. J. Biochem.* **7**:102

37. Skulachev, V. P. 1971. Energy transformations in the respiratory chain. *Curr. Top. Bioenerget.* **4**:127
38. Slayman, C. L. 1965. Electrical properties of *Neurospora crassa:* Effects of external cations on the intracellular potential. *J. Gen. Physiol.* **49**:69
39. Slayman, C. L. 1965. Electrical properties of *Neurospora crassa:* Respiration and the intracellular potential. *J. Gen. Physiol.* **49**:93
40. Slayman, C. L. 1970. Movement of ions and electrogenesis in microorganism. *Amer. Zoologist* **10**:377
41. Slayman, C. L. 1973. Adenine nucleotide levels in *Neurospora,* as influenced by conditions of growth and by metabolic inhibitors. *J. Bacteriol.* **114**:752
42. Slayman, C. L., Lu, C. Y.-H., Shane, L. 1970. Correlated changes in membrane potential and ATP concentrations in *Neurospora. Nature* **226**:274
43. Slayman, C. L., Slayman, C. W. 1968. Net uptake of potassium in *Neurospora:* Exchange for sodium and hydrogen ions. *J. Gen. Physiol.* **52**:424
44. Slayman, C. L., Slayman, C. W. 1973. H^+-dependent cotransport and the electrogenic pump in the plasma membrane of *Neurospora. Abstracts,* 73*rd Ann. Meet. Amer. Soc. Microbiol.,* Item P189
45. Slayman, C. W., Slayman, C. L. 1970. Potassium transport in *Neurospora:* Evidence for a multisite carrier at high pH. *J. Gen. Physiol.* **55**:758
46. Slayman, C. W., Tatum, E. L. 1964. Potassium transport in *Neurospora.* I. Intracellular sodium and potassium concentrations, and cation requirements for growth. *Biochim. Biophys. Acta* **88**:578
47. Slayman, C. W., Tatum, E. L. 1965. Potassium transport in *Neurospora.* II. Measurement of steady-state potassium fluxes. *Biochim. Biophys. Acta* **102**:149
48. Spanswick, R. M. 1972. Evidence for an electrogenic ion pump in *Nitella translucens.* I. The effects of pH, K^+, Na^+, light, and temperature on the membrane potential and resistance. *Biochim. Biophys. Acta* **288**:73
49. Strehler, B. L. 1965. Adenosine-5′-triphosphate and creatine phosphate. Determination with luciferase. *In:* Methods of Enzymatic Analysis. H. U. Bergemeyer, editor. p. 559. Academic Press Inc., New York
50. Tamai, T., Kagiyama, S. 1968. Studies of cat heart muscle during recovery after prolonged hypothermia. Hyperpolarization of cell membranes and its dependence on the sodium pump with electrogenic characteristics. *Circulation Res.* **22**:423
51. Thomas, R. C. 1969. Membrane current and intracellular sodium changes in a snail neurone during extrusion of injected sodium. *J. Physiol.* **201**:495
52. Thomas, R. C. 1972. Electrogenic sodium pump in nerve and muscle cells. *Physiol. Rev.* **52**:563
53. Ullrich, F. 1966. The inhibition of magnesium-activated mitochondrial adenosine triphosphatase by calcium. *Biochim. Biophys. Acta* **122**:298
54. Viotti, A., Bagni, N., Sturani, E., Alberghina, F. A. M. 1971. Magnesium and polyamine levels in *Neurospora crassa* mycelia. *Biochim. Biophys. Acta* **244**:329
55. Vogel, H. J. 1956. A convenient growth medium for *Neurospora* (Medium N). *Microbiol. Gen. Bull.* **13**:42
56. Weibull, C., Greenawalt, J. W., Löw, H. 1962. The hydrolysis of adenosine triphosphate by all fractions of *Bacillus megaterium.* I. Localization and general characteristics of the enzymatic activities. *J. Biol. Chem.* **237**:847
57. West, I. C., Mitchell, P. 1973. Stoichiometry of lactose-proton symport across the plasma membrane of *Escherichia coli. Biochem. J.* **132**:587
58. Zalokar, M. 1959. Enzyme activity and cell differentiation in *Neurospora. Amer. J. Bot.* **46**:555
59. Zalokar, M. 1959. Growth and differentiation of *Neurospora* hyphae. *Amer. J. Bot.* **46**:602